materials

MDPI

Article

Preparation, Characteristics, and Application of Bifunctional TiO_2 Sheets

Xiaoyan Guo [1,2], Jiaqi Liu [1], Lixia Liu [1], Suohe Yang [1], Guangxiang He [1] and Haibo Jin [1,2,*]

[1] College of Chemical Engineering, Beijing Institute of Petrochemical Technology, Beijing 102617, China; guoxiaoyan@bipt.edu.cn (X.G.); 2018520011@bipt.edu.cn (J.L.); liulixia@bipt.edu.cn (L.L.); yangsuohe@bipt.edu.cn (S.Y.); hgx@bipt.edu.cn (G.H.)

[2] Beijing Key Laboratory of Fuels Cleaning and Advanced Catalytic Emission Reduction Technology, Beijing 102617, China

* Correspondence: jinhaibo@bipt.edu.cn

Received: 5 March 2020; Accepted: 27 March 2020; Published: 1 April 2020

Abstract: TiO_2 is a high-reflectance material for preparing sheets during dry reagent chemical tests in detail. In this study, bifunctional TiO_2 sheets with diffusive and reflective properties were prepared using TiO_2 microspheres (particle size 2–3 μm) and cellulose acetate (CA). Factors such as the CA dosage, water content, mixing time, and the choice of surfactant were investigated. The structure and properties of the bifunctional TiO_2 sheets were characterized by thermogravimetry and differential thermal analysis (TG-DAT), scanning electron microscopy (SEM), dynamic contact angle test and reflectance spectroscopy. By studying the above experimental results, it was concluded that the most optimal preparation conditions for preparing the bi-functional TiO_2 sheets under natural drying conditions were as follows: the mass ratio of CA to TiO_2 microspheres was 0.05:1; Triton-100 was used to improve the diffusion performance of the bifunctional sheets, after mixing for 5 h and coating. The light reflectivity of the bifunctional TiO_2 sheets in the 420 to 800 nm range was higher than 90%. Serum diffused in the bifunctional TiO_2 sheets reacted in the reagent sheets and formed uniform colorful spots. Considering the repeatability of spot proportion and light reflectivity, the sheet offered a uniform serum diffusion and good repeatability. So, the bifunctional TiO_2 sheets are nominated as a promising material for dry chemical diagnostic reagents.

Keywords: TiO_2; cellulose acetate; bifunctional; sheets; dry reagent

1. Introduction

Dry reagent chemical tests, which have advantages such as long stability, decreased pollution, and easy operation compared to liquid reagents, are widely applied in clinical and food analysis. The quantification of these tests is typically carried out by using reflectance spectroscopy [1]. High-reflectance materials such as titanium dioxide, barium sulfate, zinc oxide, and lead oxide can be used to prepare reflective sheets. Porous diffusion sheets are absolutely necessary to uniformly distribute the test solution. While some commercial filter papers have been used as a diffusion sheet, they increase the test solution volume because of their water-absorbing capacity.

Of the high-reflectance materials mentioned above, TiO_2 has been extensively studied because of its great potential in several fields: photocatalysis [2,3], energy storage and conversion [4–8], and sensors [9–14]. Moreover, it has antifouling properties [15,16], antibacterial activity [17,18], and can be used for filters [19] and pigments [15,20,21]. Porous TiO_2 sheets are prepared using a papermaking technique which blends ceramic fiber with TiO_2 [22]. Both TiO_2 and S-doped TiO_2 (S-TiO_2) are immobilized on flexible low-cost aluminum sheets using a simple sol-gel dipping process [23].

Some researchers have investigated the use of TiO_2 blends in organic polymer membranes to increase its hydrophobicity. Those membranes prepared using an easy-operation and quick-preparation method have good performance on permeate flux in filtration. A study on cellulose acetate/TiO_2 hybrid membranes reported that the addition of TiO_2 nanoparticles leads to an enhanced permeate flux of water [24]. Another study on cellulose acetate butyrate/TiO_2 hybrid membranes reported that the addition of TiO_2 enhanced the rejection and permeate flux infiltration of bovine serum albumin solution [25]. Those membranes are modified organic polymer membranes with TiO_2 concentration varying from 0 to 25% [24]. However, few previous studies have been conducted to increase TiO_2 concentration over 95% even to prepare TiO_2 sheets while using less than 5% cellulose acetate as an organic polymer.

In this study, TiO_2 microspheres and a cellulose acetate solution were blended to prepare bifunctional TiO_2 sheets with diffusive and reflective properties. The properties and performance of the prepared sheets during dry reagent chemical tests were investigated in detail. The structure and properties of the TiO_2 sheet were analyzed using thermogravimetry and differential thermal analysis, scanning electron microscopy, dynamic contact angle test and reflectance spectroscopy.

2. Materials and Methods

2.1. Materials

2–3 μm TiO_2 microspheres were prepared in our own lab [26]. Cellulose acetate with an average molecular weight of 30,000 g·mol^{-1} was procured from Sino pharm Group (Beijing, China). Triton-100 (J&K Scientific, Beijing, China) was used as the surfactant. Acetone and dehydrated ethanol were procured from the Beijing reagent factory (Beijing, China), which were used as the solvent. Distilled water was used as a non-solvent. Serum was donated by Ortho-clinical Diagnostics, Inc (Rochester, NY, USA).

2.2. Sheet Preparation

Cellulose acetate (CA) solution was prepared from 1 g CA, and 12 mL acetone. Subsequently 1 g TiO_2 microspheres, 5.26 μL Triton-100, and CA solution varied mass fraction from 0.04 to 0.065 were added into the mixture. The mixture was agitated for 3 h at 350 r/min and kept at 25 °C for 5 h to remove the air bubbles.

Afterward, 300 μm thick wet sheets were cast on a glass plate using a film applicator. The cast sheets were subsequently steamed and then immersed in a 25 °C distilled water bath. Finally, the membranes were heat-treated in a 50 °C deionized water bath for 20 min to remove the excess acetone.

2.3. Sheet Characterization

2.3.1. Scanning Electron Microscopy

The top surface and cross-section of the sheets were observed with a ZEISS SUPRA55 scanning electron microscope (SUPRA-55 SEM, Zeiss, Jena, Germany) [26]. The sheets were cut into small pieces under liquid nitrogen to obtain a generally consistent and clean cut. The sheets were sputter-coated with a thin gold film and then mounted on brass plates with double-sided adhesive tape. Photomicrographs were taken in very high vacuum conditions at 5 kV.

2.3.2. Dynamic Contact Angle Test

The dynamic contact angle of the sheets was tested by an Attension C-201 (Attension C-201, Biolin Scientific, Gothenburg, Sweden) optical contact angle tester [27]. The specific operation steps were as follows: i) the sample was fixed on the test platform; ii) the droplets were dripped from the needle of the syringe onto the surface of the sample, and the dynamic value of the contact angle was read out by

the instrument through rapid photography. The liquid used in the contact angle measurement was deionized water, and the amount of water in the needle was 3 μL when measured.

2.3.3. Thermal Properties

Thermal degradation was conducted using a thermal gravimetric analyzer (SDT-Q600, TA, New Castle, PA, USA). A 25 mg sample was loaded in a pretarred platinum pan and preheated it above 120 °C to remove the moisture. After cooling to 25 °C, the sample was reheated to 700 °C at a 20 °C/min rate.

2.3.4. Water Content

The wet weights of the sheets were obtained after soaking the sheets in water for 24 h. The sheets were weighed after wiping with blotting paper. The wet sheets were placed in a vacuum drier at 75 °C for 48 h and the dry weights of the sheets were determined [12,22]. The percentage of water content (WC) was calculated using the following Equation (1):

$$WC\% = \frac{W_{wet} - W_{dry}}{W_{wet}} \times 100\% \quad (1)$$

W_{wet} and W_{dry} are the wet and dry weights of the sheets, respectively.

2.3.5. Reflection Tests

Reflection tests were performed using a UV-Vis-NIR spectrophotometer (Lambda 950, Perkin Elmer, Waltham, MA, USA) with an integral sphere (Lab sphere, 150 mm RSA ASSY) [26].

2.3.6. Diffusion Performance Tests

The reagent sheet was prepared and cut into 6 pieces, then a TiO_2 bifunctional sheet was prepared on each reagent sheet. Six 10 μL serum samples with 600 mg/dL of glucose were added onto the surface of those TiO_2 bifunctional sheets, separately, which were then batch operated at 37 °C for 10 min. When the serum diffused through the sheets and reacted in the reagent sheets, colored spots formed. The diameters of the spots and the reflection rate were determined.

The standard deviation (SD) was calculated using the following Equations (2) and (3):

$$SD\% = \sqrt{\frac{\sum_{i=1}^{n}\left(X_i - \overline{X}\right)^2}{n}} \times 100\% \quad (2)$$

$$\overline{X} = \frac{\sum_{i=1}^{n} X_i}{n} \quad (3)$$

3. Results

3.1. Analysis of TiO_2 Particles

The result of the particle size analyzer evaluation of the TiO_2 micro-particles is shown in Figure 1. As this figure shows, the average particle size of TiO_2 was equal to 2.37 μm.

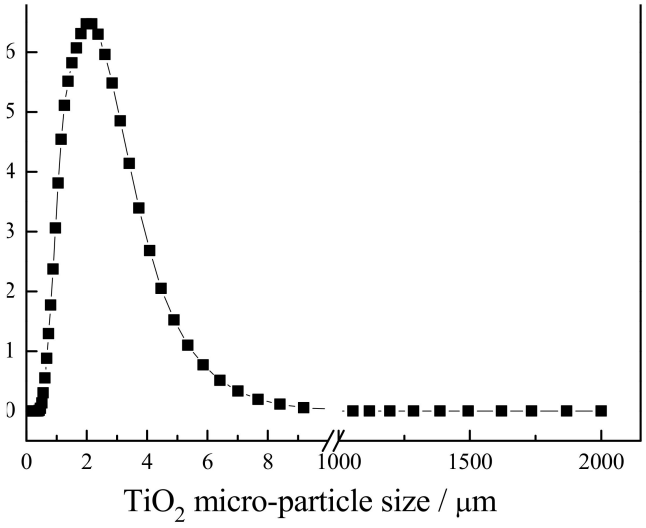

Figure 1. Particle size distribution for TiO_2 micro-particle.

3.2. Sheet Morphology

Bifunctional sheets were prepared according to the above methods. When a low mass ratio of CA to TiO_2 (0.04:1) was used, it was unable to prepare uniform sheets and the sheets broke to pieces easily. As the mass ratio increased to 0.045:1, the adhesion degree between CA and TiO_2 improves, but the sheets were still easy to crack. Using higher CA to TiO_2 mass ratios of 0.05:1, 0.06:1, and 0.065:1, the sheets formed a uniform, white, shiny monolithic laminar material as shown in Figure 2.

Figure 2. Panorama image of TiO_2 bifunctional sheets.

SEM images were used to observe the porous surface morphology and determine the effects of a CA to TiO_2 mass ratio varying from 0.05:1 to 0.06:1. The results are shown in Figure 3.

With a mass ratio of 0.05:1, the pore distribution of the TiO_2 sheets was dense and easy to present a uniform aperture size (Figure 3a). When the mass ratio increased to 0.055:1, the aperture size decreased because the TiO_2 microspheres were coated with CA. (Figure 3b). As the CA to TiO_2 mass ratio increased to 0.06:1, more TiO_2 microspheres were wrapped or more pores were filled with CA (Figure 3c). In the preparation process, acetone solvent is used to completely dissolve CA, and TiO_2 can be combined more evenly.

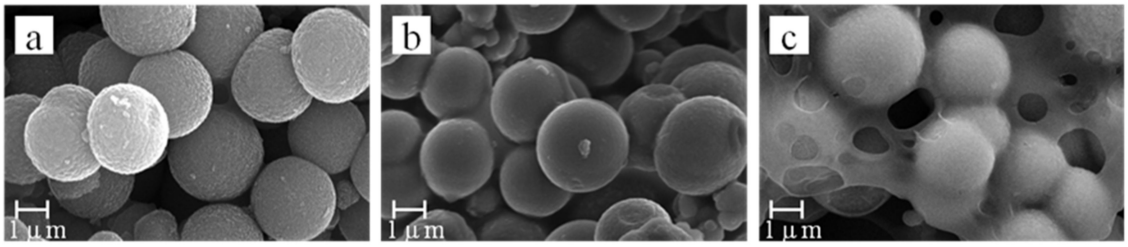

Figure 3. SEM micrographs of bifunctional TiO_2 sheets with different mass ratios of cellulose acetate (CA) and TiO_2: (**a**) 0.05:1; (**b**) 0.055:1; (**c**) 0.06:1.

The different morphologies and properties of the TiO_2 bifunctional sheets were mainly caused by the different mass ratios of CA to TiO_2. On the one hand, the effect of CA mainly showed adhesive characteristics in the system. With the mass ratio under 0.05:1, the sheets were easy to break into pieces because of poor adhesive strength with the TiO_2 microspheres; on the other hand, the excess amount of CA can wrap the TiO_2 microspheres or fill some pores which is not conducive to the diffusivity of the solution.

3.3. Contact Angle Test

Contact angle dynamic continuous test analysis was performed on the sheet. When the droplets dropped, the surface of the sheet was wetted by the liquid. Then the apparent contact angle was measured from the composite surface composed of the fluid and the solid as a baseline at 3s as shown in Figure 4. It can be seen from the test results that as the mass ratio of CA to TiO_2 increased, the diffusion of the droplets on the sheet slowed down. Therefore, with a mass ratio of 0.05:1, it can not only form uniform sheets, but also diffuse liquid rapidly.

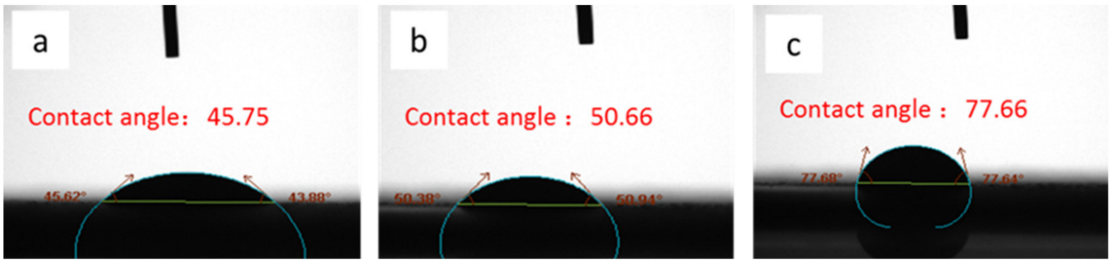

Figure 4. Dynamic contact angle test of bifunctional TiO_2 sheets with different mass ratio of CA and TiO_2 (**a**) 0.05:1; (**b**) 0.055:1; (**c**) 0.06:1.

3.4. Mixing Time

The optimum mass ratio of CA to TiO_2 is 0.05:1 to prepare casting slurry. After different mixing times, the slurry solutions were cast on a coating machine using 300 μm-thick sheet applicators, which were dried naturally. Results are shown in Figure 5.

As shown in Figure 5, the TiO_2 bifunctional sheets became smoother with longer mixing times. When mixing times were 0.5 h, 2 h, 3 h, and 4 h, separately, TiO_2 microspheres could not disperse evenly because a part of the TiO_2 microspheres agglomerated, which led to bulges on the sheets' surface (Figure 5a–e). Moreover, agglomeration led to a lower amount of CA in the bulges, which makes the sheets easily broken in the area of the bulges. As the mixing time extends to 5 h, TiO_2 microspheres evenly disperse thus the surface of sheets is smooth (Figure 5f). Consequently, to generate TiO_2 sheets with a uniform and smooth surface, the slurry mixing time should not be less than 5 h.

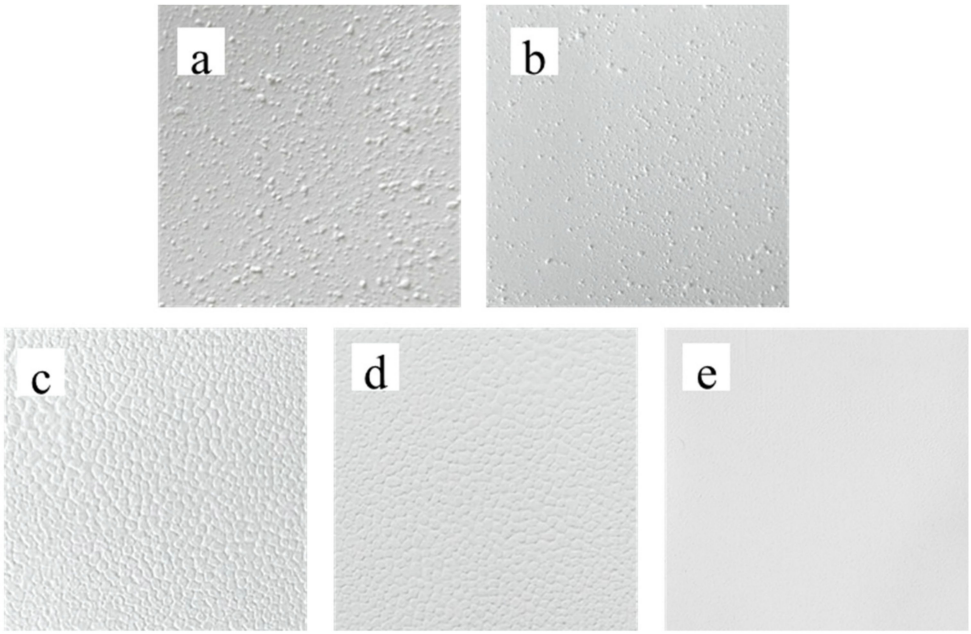

Figure 5. TiO_2 bifunctional sheets prepared at different times: (**a**) 30 min; (**b**) 2 h; (**c**) 3 h; (**d**) 4 h; (**e**) 5 h.

To investigate the dispersion effect of the TiO_2 bifunctional sheets, 10 μL serum was added to sheets prepared at different mixing times of 30 min, 2 h, 3 h, 4 h, and 5 h, respectively. As shown in Figure 6, after 10 s of diffusion, the serum could hardly diffuse on the surface of the 30 min-stirred sheets. The diffusion ability of the TiO_2 sheets prepared with 2 h stirring was slightly improved. The residual liquid on the surface decreased, but the diffusion effect was still not ideal. The serum diffused fast without any residue on the surface of sheets prepared with 5 h stirring.

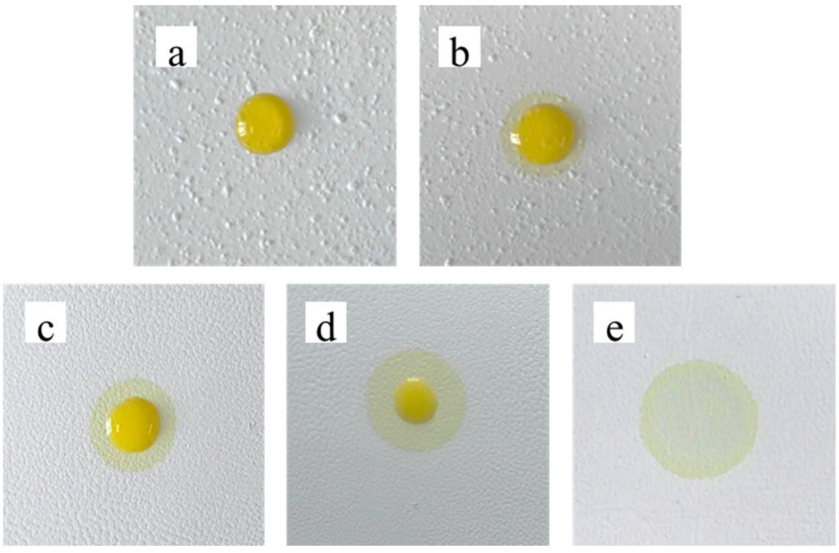

Figure 6. The diffusion of serum by TiO_2 bifunctional sheets: (**a**) 30 min; (**b**) 2 h; (**c**) 3 h; (**d**) 4 h; (**e**) 5 h.

At short stirring times, TiO_2 microspheres agglomerated which led to a lower amount of CA in the bulges, but a higher one in the flat areas and on the surface of the bulges. With a CA to TiO_2 mass ratio higher than 0.50:1, diffusion was lower as described in 3.2. As time goes on, the water in the serum evaporated and a serum sheet gradually formed on the surface of the TiO_2 bifunctional sheets,

which was more difficult to diffuse to reaction sheets. Therefore, the mixing time has a crucial influence on the diffusion effect of the serum.

3.5. Thermal Properties

The thermal analysis results of the CA/TiO_2 hybrid sheets are illustrated in Figure 7. The decomposition temperature decreased as the mass ratio of CA to TiO_2 increased because TiO_2 has better thermal stability than CA. It can be seen that the content of CA had an influence on the thermal stability of the sheets [28]. The sheets are used at room temperature or 37 °C, so it does not affect the application of the sheets.

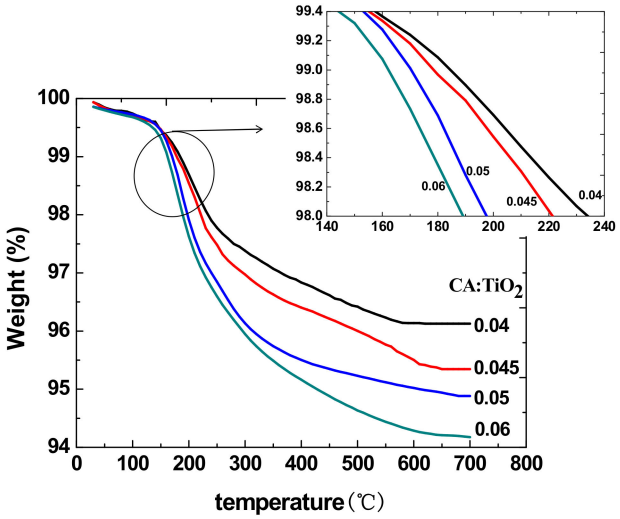

Figure 7. DTA-TG characterization of CA/TiO_2 hybrid sheets.

3.6. Water Content

Water content is related to the hydrophilic properties of the membrane [29]. The water content of each membrane was calculated using Equation (1). As shown in Table 1, the water content was measured for six sheets prepared under the same conditions. The results show that the average water content of the sheets was 57.1%, which indicates that the sheets are hydrophilic. The standard deviation is 0.01, which illustrates that the sheets had good repeatability at water content and the pore distribution between CA and the TiO_2 microspheres was uniform.

Table 1. Different water content of each sheet.

Sheets Code	W_{dry} (g)	W_{wet} (g)	WC (%)
S1	0.025	0.059	57.6%
S2	0.026	0.061	57.4%
S3	0.026	0.062	58.1%
S4	0.026	0.060	56.7%
S5	0.026	0.059	55.9%
S6	0.026	0.060	56.7%

3.7. Reflection Tests

The reflectance of the TiO_2 sheets was detected using a UV-Vis-NIR spectrophotometer and the results are shown in Figure 8.

Figure 8 shows that the light reflectivity of TiO_2 bifunctional sheets at 420 to 800 nm is higher than 90%. When CA/TiO_2 (m/m) was 0.05:1, the light reflectivity of the prepared TiO_2 sheets reached

more than 90%. Especially in the wavelength range of 540 nm (glucose detection wavelength) to 670 nm, (uric acid detection wavelength), light reflectivity even reached 94.2% and 95.7%, respectively. The light reflectivity values for a group of five samples with different amounts of CA added were all ideal; thus, small amounts of CA did not significantly affect the shading function of the TiO_2 sheets. Therefore, TiO_2 sheets with superior light-reflective properties can be used with in vitro diagnostic dry chemical reagents.

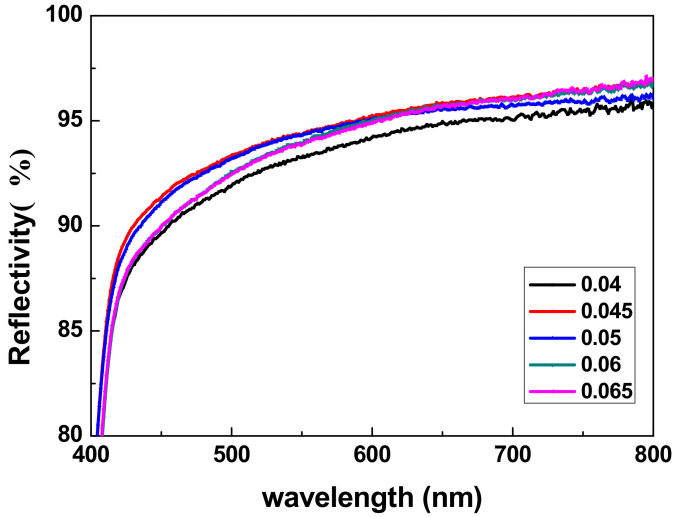

Figure 8. Light reflectivity of TiO_2 bifunctional sheet.

3.8. Chip Detection

The standard curve of the glucose detection chip at different glucose concentrations was shown in Figure 9. With increased concentration, the color reaction between glucose and detection chip was more obvious; the color gradually deepened, resulting in the corresponding light absorption value increasing. The signal value measures the light reflection, so the corresponding signal value was reduced.

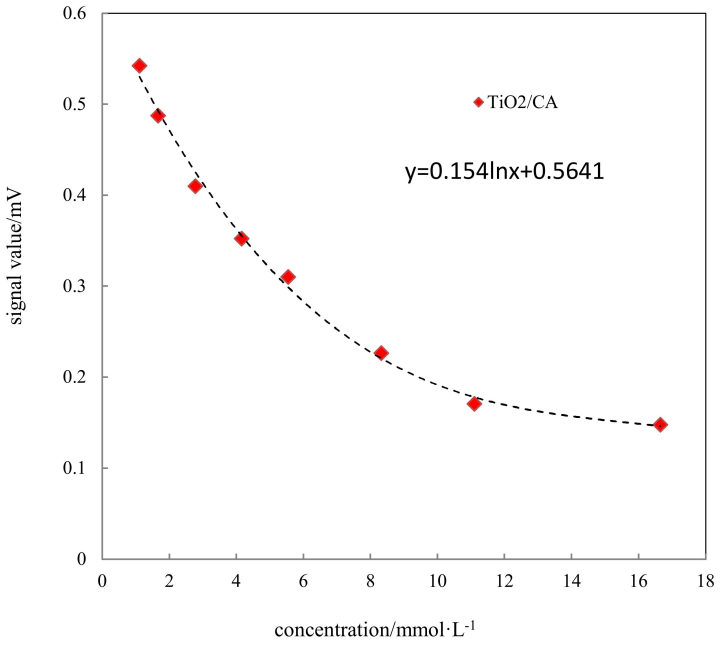

Figure 9. Standard curves of glucose detection chips.

4. Discussion

Generally, the serum was diffused by the TiO_2 bifunctional sheets and reacts with the reagent sheet with a red reaction color. To explore the reproducibility of the diffusion results for TiO_2 bifunctional sheets, the following experiments were performed.

The reagent sheet was composed of the reaction substrate enzymes. In the reagent sheet, the main reaction of glucose and reagent was as follows:

$$\beta - D - \text{glucose} + O_2 + H_2O \xrightarrow{\text{Glcose oxidase}} D - \text{gucono} + H_2O_2 \quad (4)$$

$$2H_2O_2 + 4 - \text{Antipyrine} + 1,7 - \text{Dihydroxynaphthalene} \xrightarrow{\text{Horseragish root}} \text{Red dye} \quad (5)$$

In the lab, homemade glucose dry chemical reagent sheet was covered with the TiO_2 bifunctional sheets to achieve glucose dry chemical diagnostic reagent conditions in vitro.

The chromogenic reaction results are shown in Figure 10. The light reflection density gauge detected the reflected light signal value for six points and the results are shown in Table 2.

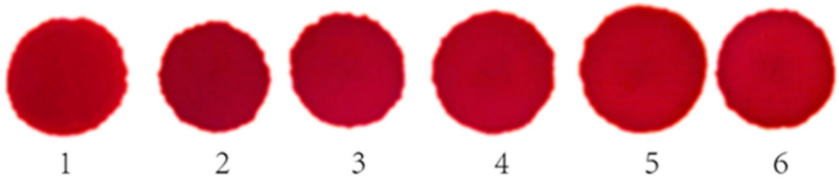

Figure 10. Spot images of serum reaction.

Table 2. Light reflection signal values of dry chemical diagnostic reagents in vitro.

Serial	Single Value (mV)	Mean Single Value	Deviation
1	88.32	88.31	0.017
2	88.32		0.017
3	88.33		0.028
4	88.28		−0.028
5	88.28		−0.028
6	88.30		−0.006

Figure 10 shows that the color of the reaction spots obtained on the reagent sheet were uniform, thus confirming that the serum diffused evenly. In addition, the areas of the six spots formed after the reaction was similar. The SD of the diameter of the six spots was 0.04, which illustrates that the sheets had good diffusion repeatability for the serum. Table 2 outlines the results for the dry chemical reagent color spots tested using reflected light density testing. The relative deviation of the light reflection signal value of the six groups ranged within ±0.028%, which illustrates that the dry chemical reagent has good reproducibility. Therefore, using the same reagent sheet for the same batch, the sheets had good serum diffusivity and an excellent repeatability.

The above results indicate that the homemade TiO_2 sheets had uniform pore distribution and aperture size on the surface, as well as inside. Therefore, TiO_2 bifunctional sheets can be further used in dry chemical diagnostic reagents tests in vitro.

5. Conclusions

(1) The most optimal preparation condition for the bifunctional TiO_2 sheets under natural drying conditions are as follows: 0.05:1 CA/TiO_2 mass ratio, 5 h mixing after coating, and natural dried.

(2) The reflection spectrometry detection results show that the reflectivity of TiO_2 bifunctional sheets between 420 and 800 nm can reach more than 90%, which is enough to prove that the prepared

sheets have a good function of reflection. The TG-DTA analysis results show that CA disperses evenly in the TiO_2 bifunctional sheets.

(3) The bifunctional TiO_2 sheets are applied to dry chemical in vitro diagnostic reagents prepared using dry glucose films. The test results confirm that the spot color is uniform when the bifunctional sheets are used for the same serum concentration. The SD for the diameter of six spots is 0.04, which illustrates that the sheets have good diffusion repeatability for the serum. The relative deviation of the light reflection signal value in the six groups range within ±0.028%, which illustrates that the dry chemical reagent had a very good reproducibility. Therefore, from the preliminary results obtained, bifunctional TiO_2 sheets are ideal to be applied to dry chemical in vitro diagnostic reagents.

Author Contributions: Conceptualization, X.G. and H.J.; methodology, X.G. and L.L.; software, J.L., S.Y. and G.H.; investigation, X.G. and L.L.; resources, X.G. and L.L.; data curation, X.G. and L.L.; writing—original draft preparation, L.L.; writing—review and editing, X.G.; supervision, H.J.; project administration, H.J. All authors have read and agreed to the published version of the manuscript.

Funding: This research was funded by the National Natural Science Foundation of China (91634101) and The Project of Construction of Innovative Teams and Teacher Career Development for Universities and Colleges under Beijing Municipality (IDHT20180508).

Conflicts of Interest: The authors declare that there is no conflict of interest.

References

1. Fujishima, A.; Honda, K. Electrochemical photolysis of water at a semiconductor electrode. *Nature* **1972**, *238*, 37–38. [CrossRef]
2. Asahi, R.; Morikawa, T.; Ohwaki, T. Visible-light photocatalysis in nitrogen-doped titanium oxides. *Science* **2001**, *293*, 269–271. [CrossRef]
3. Yang, H.G.; Sun, C.H.; Qiao, S.Z. Anatase TiO_2 single crystals with a large percentage of reactive facets. *Nature* **2008**, *453*, 638–641. [CrossRef]
4. Yu, X.; Wang, H.; Liu, Y. One-step ammonia hydrothermal synthesis of single crystal anatase TiO_2 nanowires for highly efficient dye-sensitized solar cells. *J. Mater. Chem. A* **2013**, *1*, 2110–2117. [CrossRef]
5. Liu, B.; Aydil, E.S. Growth of oriented single-crystalline rutile TiO_2 nanorods on transparent conducting substrates for dye-sensitized solar cells. *J. Am. Chem. Soc.* **2009**, *131*, 3985–3990. [CrossRef]
6. Feng, X.; Shankar, K.; Varghese, O.K. Vertically aligned single crystal TiO_2 nanowire arrays grown directly on transparent conducting oxide coated glass: Synthesis details and applications. *Nano Lett.* **2008**, *8*, 3781–3786. [CrossRef]
7. Ye, J.; Liu, W.; Cai, J. Nanoporous anatase TiO_2 mesocrystals: Additive-free synthesis, remarkable crystalline-phase stability, and improved lithium insertion behavior. *J. Am. Chem. Soc.* **2011**, *133*, 933–940. [CrossRef]
8. Chen, J.S.; Wang, Z.; Dong, X.C. Graphene-wrapped TiO_2 hollow structures with enhanced lithium storage capabilities. *Nanoscale* **2011**, *3*, 2158–2161. [CrossRef]
9. Kim, I.D.; Rothschild, A.; Lee, B.H. Ultrasensitive chemiresistors based on electrospun TiO_2 nanofibers. *Nano Lett.* **2006**, *6*, 2009–2013. [CrossRef]
10. Varghese, O.K.; Gong, D.; Paulose, M. Hydrogen sensing using titania nanotubes. *Sensor Actuat B-Chem.* **2003**, *93*, 338–344. [CrossRef]
11. Comini, E.; Faglia, G.; Sberveglieri, G. Stable and highly sensitive gas sensors based on semiconducting oxide nanobelts. *Appl. Phys. Lett.* **2002**, *81*, 1869–1871. [CrossRef]
12. Fields, L.L.; Zheng, J.P.; Cheng, Y. Room-temperature low-power hydrogen sensor based on a single tin dioxide nanobelt. *Appl. Phys. Lett.* **2006**, *88*, 263102. [CrossRef]
13. Patolsky, F.; Zheng, G.; Lieber, C.M. Fabrication of silicon nanowire devices for ultrasensitive, label-free, real-time detection of biological and chemical species. *Nat. Protoc.* **2006**, *1*, 1711–1724. [CrossRef]
14. Patolsky, F.; Zheng, G.; Lieber, C.M. Nanowire-based biosensors. *Anal. Chem.* **2006**, *78*, 4260–4269. [CrossRef]
15. Zhang, X.T.; Sato, O.; Taguchi, M.; Einaga, Y.; Murakami, T.; Fujishima, A. Self-cleaning particle coating with antireflection properties. *Chem Mater.* **2005**, *17*, 696–700. [CrossRef]
16. Parkin, I.P.; Palgrave, R.G. Self-cleaning coatings. *Surf. Eng.* **2005**, *25*, 89–92. [CrossRef]

17. Necula, B.S.; Fratila-Apachitei, L.E.; Zaat, S.A. In vitro antibacterial activity of porous TiO_2-Ag composite layers against methicillin-resistant Staphylococcus aureus. *Acta Biomater.* **2009**, *5*, 3573–3580. [CrossRef]
18. Marciano, F.R.; Limaoliveira, D.A.; Dasilva, N.S. Antibacterial activity of DLC films containing TiO_2 nanoparticles. *J. Colloid Inter. Sci.* **2009**, *340*, 87–92. [CrossRef]
19. Sabbah, H. Amorphous titanium dioxide ultra-thin films for self-cleaning surfaces. *Mater. Express.* **2013**, *3*, 171–175. [CrossRef]
20. Peng, B.; Tang, F.; Chen, D. Preparation of PS/TiO_2/UF multilayer core-shell hybrid microspheres with high stability. *J. Colloid Inter. Sci.* **2009**, *329*, 62–66. [CrossRef]
21. Choi, H.C.; Jung, Y.M.; Kim, S.B. Size effects in the Raman spectra of TiO_2, nanoparticles. *Vib. Spectrosco.* **2005**, *37*, 33–38. [CrossRef]
22. Fukahori, S.; Ichiura, H.; Kitaoka, T.; Tanaka, H.; Wariishi, H. Preparation of porous sheet composite impregnated with TiO 2photocatalyst by a papermaking technique. *J. Mater. Sci.* **2007**, *42*, 6087–6092. [CrossRef]
23. Wang, Y.; Du, G.; Liu, H. Nanostructured sheets of TiO_2 nanobelts for gas sensing and antibacterial applications. *Adv. Funct. Mater.* **2008**, *18*, 1131–1137. [CrossRef]
24. Abedini, R. A novel cellulose acetate (CA) membrane using TiO_2 nanoparticles: Preparation, characterization and permeation study. *Desalination* **2011**, *277*, 40–45. [CrossRef]
25. Asgarkhani, M.A.H.; Mousavi, S.M.; Saljoughi, E. Cellulose acetate butyrate membrane containing TiO_2 nanoparticle: Preparation, characterization and permeation study. *Korean J. Chem. Eng.* **2013**, *30*, 1819–1824. [CrossRef]
26. Guo, X.Y.; Li, Y.; Zhen, Y. Synthesis and characterization of homogeneous titanium dioxide microspheres. *Fine Chem.* **2017**, *34*, 1404–1411.
27. Lai, S.O.; Heng, S.L.; Chong, K.C. Deacidification of palm oil using solvent extraction integrated with membrane technology. *Jurnal Teknologi* **2016**, *78*, 69–74. [CrossRef]
28. Bae, T.H.; Kim, I.C.; Tak, T.M. Preparation and characterization of fouling-resistant TiO_2 self-assembled nanocomposite membranes. *J. Membr. Sci.* **2006**, *275*, 1–5. [CrossRef]
29. Sivakumar, M.; Mohan, D.R.; Rangarajan, R. Studies on cellulose acetate-polysulfone ultrafiltration membranes: II. Effect of additive concentration. *J. Membr. Sci.* **2006**, *268*, 208–219. [CrossRef]